applied sciences

MDPI

Article

Application Research of Multi-Mode Relay in Future Heterogeneous Networks

Wenle Bai [1,*,†], Yu Xiao [2,†], Danping Hu [3] and Yongmei Zhang [1]

1 School of Information, North China University of Technology, Beijing 100144, China; zhangym@ncut.edu.cn
2 Wireless Theory and Technology Lab (WT&T), Beijing University of Posts and Telecommunications Beijing, Beijing 100876, China; xy_1st@163.com
3 Is an Independent Researcher; danpinghu19@gmail.com
* Correspondence: bwl@ncut.edu.cn
† These authors contributed equally to this work.

Received: 25 July 2019; Accepted: 6 September 2019; Published: 19 September 2019

Abstract: The fast increase of users in existing mobile networks requires more base stations (BSs) to bear more communication traffic. Future heterogeneous network is considered to be a promising candidate architecture to meet the demands of wireless networks under scarcity of radio frequency (RF) resources. In this paper, we present a multi-mode relay (MMR) model based on two-way relay technology, which is applied to heterogeneous hierarchical wireless networks (HHWN), and set up a system model of HHWN with 3 tiers, 2 users between the macrocell, and the picocell as the multi-mode relay (MMR). Specifically, we consider the new system with unequal relay emission power situation, which is usually researched in the traditional literature with equal relay emission powers. Based on this idea, we define the two-way SINR ratio, derive the mathematical formulas of outage error probability with channel estimation errors, and verify theoretical expressions by data simulations. For further comparison, several experiments are implemented to illuminate the effect on outage probability among different levels of relay emission power, noise power, and signal power. Furthermore, several conclusions are obtained, which have some meanings for implementing MMR in future heterogeneous networks.

Keywords: heterogeneous wireless networks; MMR; unequal relay power; outage probability

1. Introduction

With the fast growth of mobile terminals, traffic of mobile data communication is growing extremely fast, which is becoming one of the challenges of network capacity and transport rate of community networks. Traditional cellular networks will soon become incapable of addressing these problems effectively. Massive multi-imput multi-output (massive MIMO) is believed to be a significant approach to meet the massive growth in data traffic. However, the growing number of antennas increases hardware cost dramatically, especially regarding the overheads of radio frequency (RF) links. There are many researchers focusing on the analog beamforming technique to decrease RF resources [1–3]. These techniques need extra computational cost at both transceiver sides. Heterogeneous hierarchical wireless networks are also considered to be an important architecture candidate to meet the demands of wireless networks in the future, due to the scarcity of RF resources [4].

5G network architecture is a perfect example of future heterogeneous hierarchical wireless networks that guarantee the user reliability and integrity [5,6]. Usually a 5G heterogeneous network manages all sorts of networks by using software-defined virtual intelligent network systems. Network function visualization (NFV) represents a significant transformation for telecommunications/service-provider networks, driven by the goals of reducing cost, increasing flexibility, and providing personalized

services. Software-defined network (SDN) is suggested to control, initialize, manage, and change network behavior automatically by opening interfaces and abstraction of lower-level functionality programmatically.

As is shown in Figure 1, heterogeneous hierarchical wireless networks (HHWN) introduces a lot of low-power base stations, such as picocells, femtocells, and distributed antenna systems (remote radio heads, such as relays). These heterogeneous elements can not only increase the flexibility of the network, but also fulfill huge user requirements for random complex data traffic, and raise its quality of service.

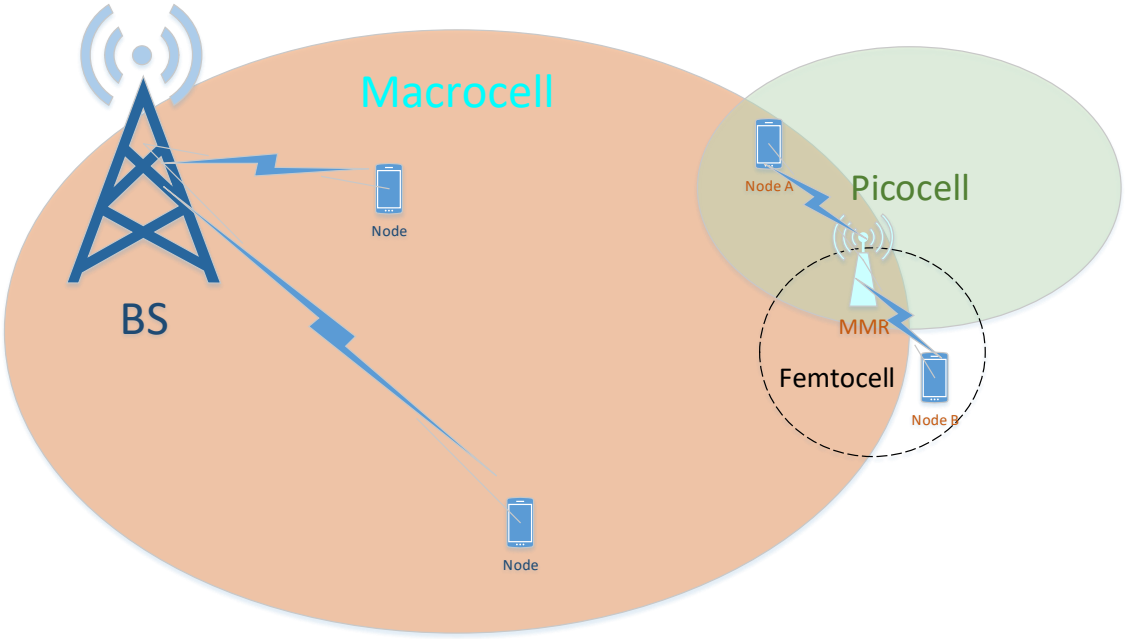

Figure 1. Multi-mode relay (MMR) running in the modes of picocell BS and femtocell BS.

Studies have been done to improve the ability of the HHWN. In [7] the hybrid grid routing protocol (HGRP) is used to take on the cost advantages of routing and energy consumption. To cope with the handover management and co-channel interference, by combining cloud ratio access network with small cells, a novel network architecture is proposed in [8], applying an effective CoMP clustering scheme to mitigate cell edge user interference. To save system energy, reference [9] showed an energy-efficient approach, and the use of heterogeneous-aware enhanced hierarchical clusters (HEHC) can obtain better energy availability. To handle the problem of cross-tier interference in spectrum-sharing deployment, Zhang et al. presented a resource-allocation scheme [10], set up a model for the sub-channel and power allocation, and presented an iterative sub-channel and power-allocation algorithm. To cope with the problem of severe inter-cell interference when we increase the wireless network capacity, reference [11] investigated the coexistence problems of sharing an unlicensed spectrum between Wi-Fi and 4G cellular networks, and proposed a new scheme to avoid interference based on estimating the density of Wi-Fi access points near small cells. To improve system reliability, reference [12] indicated that a resource management unit can be introduced into HHWN to implement the distributed grids, then proposed a semi-centralized hierarchical architecture to balance the load of HHWN.

The increase of the low-power base stations may result in inconvenience since a lot of base stations are equipped in a certain area. There may even appear the complex situation that multi-BSs (picocell, femtocell) and multi-HotPoints (wireless router, Wi-Fi relay) coexist, especially at the edge of a macrocell. To solve the aforementioned problems, we unify two or more kinds of BSs to one single piece of equipment. This makes us consider that emission powers of different kinds of BSs are different.

Accordingly, we provide equipment that can produce different powers to cater to different levels of HHWN. Multi-Mode Relay (MMR), in brief, has different modes of emission powers, which is out of ordinary relay at present. We may consider that the base station in the picocell and femtocell, which is at the edge of the macrocell, could be represented as relays, as shown in Figure 1. Because of the different transmission power in the base stations of different layers, the relay must use more than two modes if it wants to integrate the picocell station and the femtocell station. In other words, the relay is not only the picocell BS, but also the femtocell BS. Consequently, the different coverage area of the cell served by MMR leads to the different transmitting power required. Then, unequal relay power problems need to be studied with extreme urgency.

Literature [13] indicated the system performance of equal relay power, because the serving nodes are considered in same layer of wireless network. However, in heterogeneous networks, especially in HHWN system, the powers of relay to UE nodes are usually different, since UE nodes are in different layer of HHWN, as mentioned above. Therefore, the main contribution of this paper is that we propose the unequal transmitting power structure in a HHWN system and derive the expression of outage probability in this structure. We also apply our expression to the system-level simulation to research system performance of future heterogeneous networks with unequal relay powers to each UE nodes.

The following parts of the paper are organized as follows. Section 2 describes the system model of a heterogeneous hierarchical wireless networks (HHWN) with multi-mode relay system model, defines the two amplify-and-forward (AF) factors for different transmission power of MMR, sets up the comparison of SINRs f_{AB} and f_{BA}, and analyzes the relationship with the MMR power, which is the key point of performance analysis. In Section 3, we consider the system with unequal relay emission powers situations, get the mathematic computation formulas of outage error probability with channel estimation errors with the conditions of different relay powers and channel state information, and give theoretical analysis. In Section 4, we present the theory computation and simulation demonstrations.

2. System Model

The HHWN system max SINR downlink coverage regions are shown in Figure 2. Every base station in the macrocell, picocell, and femtocell can be represented as the relay in MMR. Because of the different transmission powers in the base station of different layers, the relay must have more than two modes if it must represent the BSs. In other words, the relay is not only the picocell BS but also the femtocell BS, which is why we call it MMR. The MMR helps node A and node B complete the communication. The MMR model is defined in Figure 3. The communication inside the MMR is not considered here. The emission powers of the two nodes in MMR equal to p_s, the relay power of MMR is p_r, and the noises of two source nodes are AWGN with zero mean and unit variance. There are limited N interferences at MMR. In this condition, the received signal at MMR is written in Equation (1), according to [14,15].

$$\mathbf{y_r} = \sqrt{p_s}\mathbf{x_A}\mathbf{H}_A + \sqrt{p_s}\mathbf{x_B}\mathbf{H}_B + \sum_{n=1}^{N}\sqrt{p_{I,n}}\mathbf{s_n}\mathbf{H}_{I,n} + \mathbf{n_r} \quad (1)$$

where $\mathbf{H}_A$ and $\mathbf{H}_B$ are the channel fading $p_{I,n}$, $\mathbf{s_n}$ is the power of nth interference signal, and $\mathbf{H_{I,n}}$ is the channel fading of nth interference signal. $\mathbf{n_r}$ is Gaussian noise with zero mean and variance of σ_r^2. As the TDD system has channel symmetry, the channel fading between MMR and i are identical.

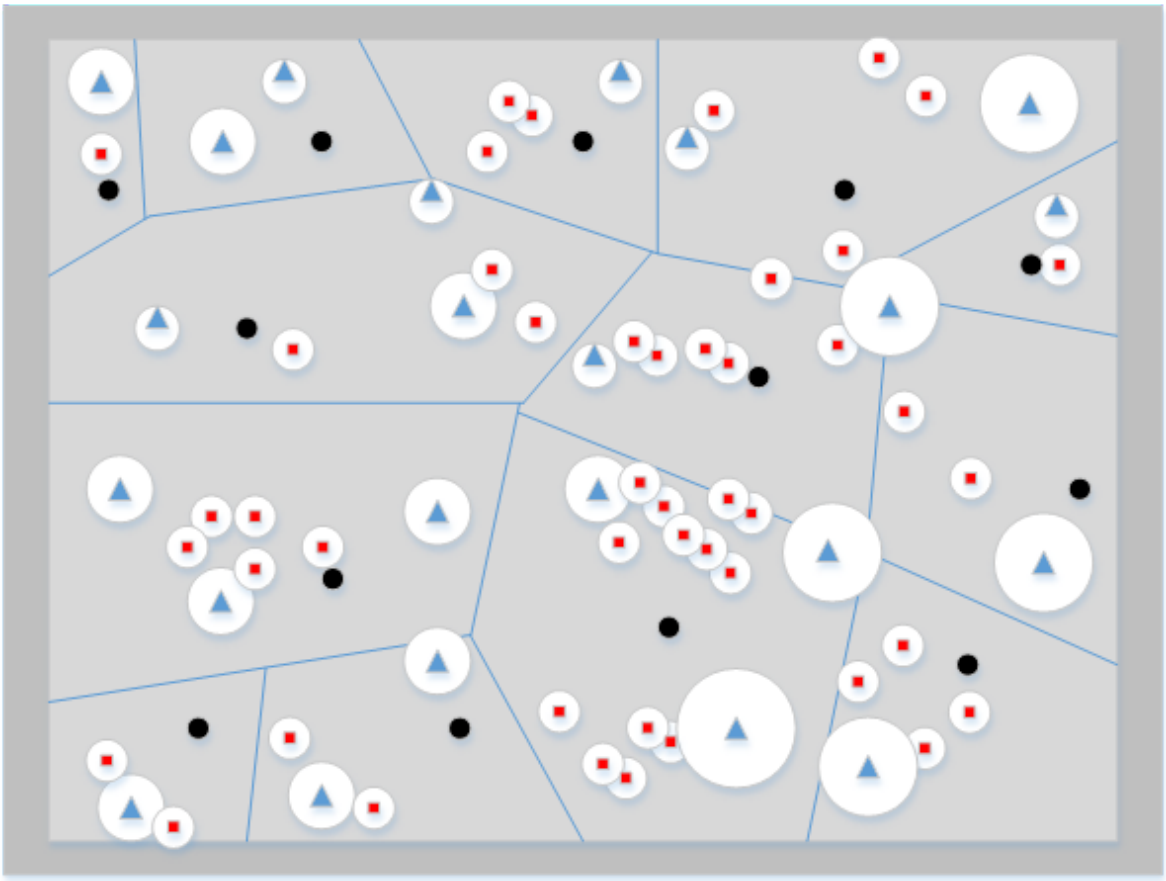

Figure 2. 3-tier HHWN max SINR downlink coverage regions with macrocells, picocells, and femtocells.

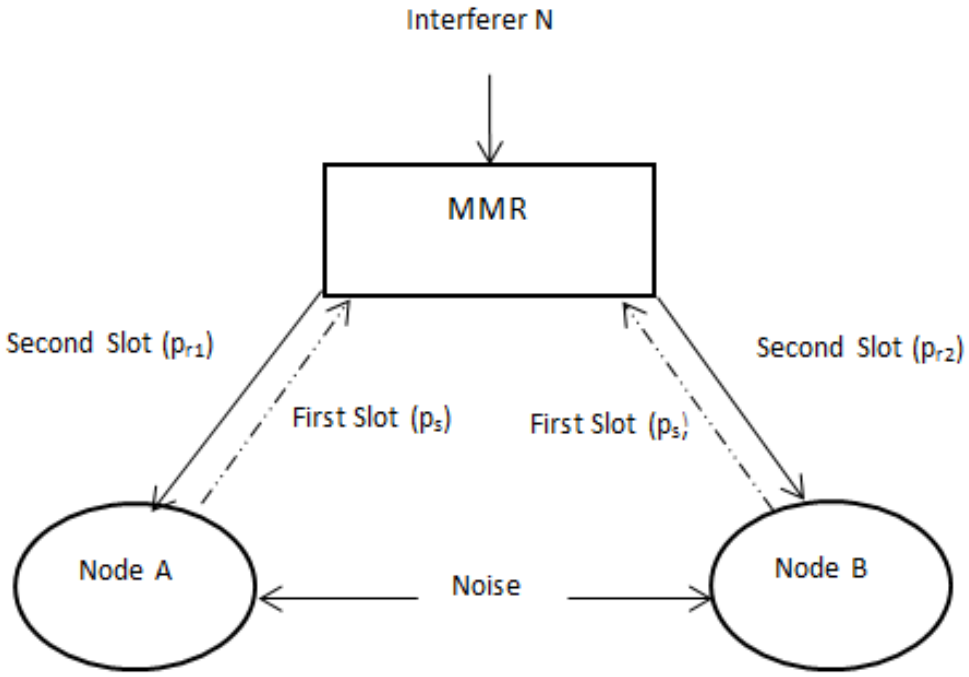

Figure 3. System model of multi-mode relay $p_{r1} \neq p_{r2}$.

In the first time slot to communicate, two nodes of A and B transmit their signal to MMR respectively, so the received signal at MMR is y_r; in the second slot, after processing, MMR relay signals back to A node and B node in two ways, and due to the multi-mode of relay, the emission power of A and B is different, respectively p_{r1} and p_{r2}. In fact, node A and B cannot achieve the best CSI, so the channel fading is modeled as

$$\mathbf{H_A} = \widetilde{\mathbf{H}}_\mathbf{A} + \mathbf{e_A} \tag{2}$$

$$\mathbf{H_B} = \widetilde{\mathbf{H}}_\mathbf{B} + \mathbf{e_B} \tag{3}$$

here $\mathbf{e_A}$ and $\mathbf{e_B}$ are deviation of the channel estimation, and make $E(|\mathbf{e_A}|) = E(|\mathbf{e_B}|) = \delta_E^2$; provided that $\tilde{\mathbf{H}}_A$ and $\tilde{\mathbf{H}}_B$ both are independent of $\mathbf{e_A}$ and $\mathbf{e_B}$ with the variances $\mu^2 = 1 - \delta_E^2$. Equations (2) and (3) are extensively used in the literature [16].

Considering the difference of the transmission power of MMR, the amplifying-and-forward (AF) factors β_s which are used in MMR could be different from the traditional amplifying factor. Combining the amplifying factor in [14], the new normalized β_s can be denoted by

$$\beta_1 = \sqrt{p_{r1} \Big/ \begin{bmatrix} p_s\left(\left|\tilde{\mathrm{H}}_A\right|^2 + \left|\tilde{\mathrm{H}}_B\right|^2\right) \\ +2p_s\sigma_E^2 + \sum_{n=1}^{N} p_{I,n}|\mathbf{H}_{I,n}|^2 \end{bmatrix}} \tag{4}$$

$$\beta_2 = \sqrt{p_{r2} \Big/ \begin{bmatrix} p_s\left(\left|\tilde{\mathrm{H}}_A\right|^2 + \left|\tilde{\mathrm{H}}_B\right|^2\right) \\ +2p_s\sigma_E^2 + \sum_{n=1}^{N} p_{I,n}|\mathbf{H}_{I,n}|^2 \end{bmatrix}} \tag{5}$$

Note that in [17], it is complex for MMR to identify between source signals and interferences. Consequently, the MMR normalizes the received signals and relays them, then the two sources A and B receive signals, which are expressed by Equations (6) and (7).

$$\begin{aligned} \mathbf{y_a} &= \sqrt{p_S}\beta_1\mathbf{H}_A^2\mathbf{x_A} + \sqrt{p_S}\beta_1\mathbf{H}_A\mathbf{H}_B\mathbf{x_B} \\ &+\beta_1\mathbf{H}_A\sum_{n=1}^{N}\sqrt{p_{I,n}}\mathbf{s_n}\mathbf{H}_{I,n} + \mathbf{N_A} \end{aligned} \tag{6}$$

$$\begin{aligned} \mathbf{y_b} &= \sqrt{p_S}\beta_2\mathbf{H}_B^2\mathbf{x_B} + \sqrt{p_S}\beta_2\mathbf{H}_A\mathbf{H}_B\mathbf{x_A} \\ &+\beta_2\mathbf{H}_B\sum_{n=1}^{N}\sqrt{p_{I,n}}\mathbf{s_n}\mathbf{H}_{I,n} + \mathbf{N_B} \end{aligned} \tag{7}$$

Here $\mathbf{N_A}$ and $\mathbf{N_B}$ are AWGN at two sources. It is assume that we have perfect channel estimation, therefore the resulting self-interference in Equations (6) and (7) can be eliminated accordingly; the received signals at sources A and B can be rewritten in Equations (8) and (9).

$$\begin{aligned} \mathbf{y_a} &= \sqrt{p_S}\beta_1\tilde{\mathbf{H}}_A\tilde{\mathbf{H}}_B\mathbf{x_B} + \sqrt{p_S}\beta_1\left(\tilde{\mathbf{H}}_A e_B + \tilde{\mathbf{H}}_B\mathbf{e_A} + \mathbf{e_A}\mathbf{e_B}\right)\mathbf{x_B} \\ &+ \sqrt{p_S}\beta_1\left(2\tilde{\mathbf{H}}_A\mathbf{e_A} + \mathbf{e_A^2}\right)\mathbf{x_A} + \beta_1\left(\tilde{\mathbf{H}}_A + \mathbf{e_A}\right)\sum_{n=1}^{N}\sqrt{p_{I,n}}s_n\mathbf{H}_{I,n} + \mathbf{N_A} \end{aligned} \tag{8}$$

$$\begin{aligned} \mathbf{y_b} &= \sqrt{p_S}\beta_2\tilde{\mathbf{H}}_A\tilde{\mathbf{H}}_B\mathbf{x_A} + \sqrt{p_S}\beta_2\left(\tilde{\mathbf{H}}_A\mathbf{e_B} + \tilde{\mathbf{H}}_B\mathbf{e_A} + \mathbf{e_A}\mathbf{e_B}\right)\mathbf{x_A} \\ &+ \sqrt{p_S}\beta_2\left(2\tilde{\mathbf{H}}_B\mathbf{e_B} + \mathbf{e_B^2}\right)\mathbf{x_B} + \beta_2\left(\tilde{\mathbf{H}}_B + \mathbf{e_B}\right)\sum_{n=1}^{N}\sqrt{p_{I,n}}\mathbf{s_n}\mathbf{H}_{I,n} + \mathbf{N_B} \end{aligned} \tag{9}$$

Here the right item next to Equations (8) and (9) is the terms of signal, noise, and interference, respectively. Accordingly, two sources SINR of A and B can be calculated by expressions of Equations (10) and (11).

$$f_A = \frac{p_s p_{r1} \left|\tilde{\mathbf{H}}_A\right|^2 \left|\tilde{\mathbf{H}}_B\right|^2}{p_s\left(p_{r1}\sigma_E^2+1\right)\left(\left|\tilde{\mathbf{H}}_A\right|^2+\left|\tilde{\mathbf{H}}_B\right|^2\right)+4p_s p_{r1}\sigma_E^2\left|\tilde{\mathbf{H}}_A\right|^2+\left(p_{r1}\left|\tilde{\mathbf{H}}_A\right|^2+p_{r1}\sigma_E^2+1\right)\sum_{n=1}^{N} p_{I,n}|\mathrm{H}_{I,n}|^2+2p_s\sigma_E^2+2p_s p_{r1}\sigma_E^4} \tag{10}$$

$$f_B = \frac{p_s p_{r2} \left|\tilde{\mathbf{H}}_A\right|^2 \left|\tilde{\mathbf{H}}_B\right|^2}{p_s\left(p_{r2}\sigma_E^2+1\right)\left(\left|\tilde{\mathbf{H}}_A\right|^2+\left|\tilde{\mathbf{H}}_B\right|^2\right)+4p_s p_{r2}\sigma_E^2\left|\tilde{\mathbf{H}}_B\right|^2+\left(p_{r2}\left|\tilde{\mathbf{H}}_B\right|^2+p_{r2}\sigma_E^2+1\right)\sum_{n=1}^{N} p_{I,n}|\mathbf{H}_{I,n}|^2+2p_s\sigma_E^2+2p_s p_{r2}\sigma_E^4} \tag{11}$$

Let $H_a = \left|\tilde{\mathbf{H}}_A\right|^2$, $H_b = \left|\tilde{\mathbf{H}}_B\right|^2$, $\mathrm{M} = \sum_{n=1}^{N} p_{I,n}|h_{I,n}|^2$, Equations (10) and (11) can be rewritten as Equations (12) and (13)

$$f_{BA} = \frac{p_s H_a H_b}{p_s\sigma_E^2(H_a+H_b)+4p_s\sigma_E^2 H_a+(H_a+\sigma_E^2)\mathrm{M}+2p_s\sigma_E^4+\frac{p_s(H_a+H_b)+\mathrm{M}+2p_s\sigma_E^2}{p_{r1}}} \tag{12}$$

$$f_{AB} = \frac{p_s H_a H_b}{p_s\sigma_E^2(H_a+H_b)+4p_s\sigma_E^2 H_b+(H_b+\sigma_E^2)\mathrm{M}+2p_s\sigma_E^4+\frac{p_s(H_a+H_b)+\mathrm{M}+2p_s\sigma_E^2}{p_{r2}}} \tag{13}$$

As shown in Formulas (12) and (13), the SINR is in direct proportion to the MMR power p_{ri} (i = 1, 2); the absolute value of channel coefficient $\mathbf{H}_A$ and $\mathbf{H}_B$ also has the influence on SINR.

3. Outage Probability Expression Derivation and Analysis

The outage events in the communication system can be denoted as: if the data rate falls below the threshold rate, the outage event of communication happens. The data rates between A and B are defined as B∼A: $F_{BA} = 0.5\log_2(1+f_{BA})$, A∼B: $F_{AB} = 0.5\log_2(1+f_{AB})$, respectively. The size of SINR is related to MMR powers (p_{r_1} and p_{r_2}) and channel conditions (H_a and H_b). If there is not any data rate which is lower than the threshold rate F_{th}, it means both rates are greater than the threshold rate F_{th}, at this time, the communication system does not have an outage event. Motivated by this, the system outage probability can be expressed as in [18].

$$\begin{aligned} P_{out} &= \Pr\{\min(F_{AB}, F_{BA}) < F_{th}\} = 1 \\ &- \Pr(f_{BA} > f_{th}, f_{AB} > f_{th}) \end{aligned} \tag{14}$$

where $f_{th} = 2^{2F_{th}} - 1$. Because of the SINR f is related to MMR power p_{r_i} (i = 1, 2), and the two p_r are independent to each other, so Formula (14) can be rewritten as Equation (15). For convenience in the further derivation, we define a factor k, let $k = \frac{f_{BA}}{f_{AB}}$, substituting Equations (12) and (13) into k, then have Equation (16).

$$\begin{aligned} P_{out} &= 1 - \Pr(f_{BA} > f_{th} | f_{BA} < f_{AB}) - \Pr(f_{AB} > f_{th} | f_{BA} > f_{AB}) \\ &= 1 - \mathrm{Pr}_1 \ - \mathrm{Pr}_2 \end{aligned} \tag{15}$$

$$k = \frac{p_s\sigma_E^2(H_a+H_b)+4p_s\sigma_E^2 H_b+\left(H_b+\sigma_E^2\right)\mathrm{M}+2p_s\sigma_E^4+\frac{p_s\left(H_a+H_b\right)+\mathrm{M}+2p_s\sigma_E^2}{p_{r2}}}{p_s\sigma_E^2(H_a+H_b)+4p_s\sigma_E^2 H_a+\left(H_a+\sigma_E^2\right)\mathrm{M}+2p_s\sigma_E^4+\frac{p_s\left(H_a+H_b\right)+\mathrm{M}+2p_s\sigma_E^2}{p_{r1}}} \tag{16}$$

After simplifying Equation (16), we get Equation (17).

$$k = \frac{\Theta + \omega H_b + p_{r1}\zeta}{\Theta + \omega H_a + p_{r2}\zeta} \tag{17}$$

where

$\Theta = p_{r1}p_{r2}\sigma_E^2\left[p_s\left(H_a + H_b\right) + \mathrm{M} + 2p_s\sigma_E^2\right]$

$\omega = \left(4p_s\sigma_E^2 + \mathrm{M}\right)p_{r1}p_{r2}$

$\zeta = p_s\left(H_a + H_b\right) + \mathrm{M} + 2p_s\sigma_E^2$

Obviously, k is relevant with p_{r1}, p_{r2} and H. In the following research derivation on MMR, we let $p_{r1} > p_{r2}$,

(1) When $H_a < H_b$, it is obvious that $k > 1$, then $f_{BA} > f_{AB}$. So

$$Pr_2{}' = \Pr\left(f_{AB} > f_{th} | H_b > H_a\right) \tag{18}$$

(2) When $H_a > H_b$, we divide two situations to further study:

(a) If $H_a \gg H_b$, overcomes the influence of $p_{r1} > p_{r2}$, then $k < 1$,$f_{BA} < f_{AB}$. What is the relationship between H_a and H_b? We let $k < 1$, then get Equation (19)

$$\left(1 - \frac{p_s}{\omega}\left(p_{r1} - p_{r2}\right)\right)H_a > \left(1 + \frac{p_s}{\omega}\left(p_{r1} - p_{r2}\right)\right)H_b + \frac{\mathrm{M}+2p_s\sigma_E^2}{\omega}\left(p_{r1} - p_{r2}\right) \tag{19}$$

Making the simplification by substituting $k_1 = \frac{p_s}{\omega}\left(p_{r1} - p_{r2}\right)$ and $k_2 = \frac{\mathrm{M}+2p_s\sigma_E^2}{\omega}\left(p_{r1} - p_{r2}\right)$ into Equation (15), and if $1 - k_1 > 0$, we get $H_a > \frac{1+k_1}{1-k_1}H_b + \frac{k_2}{1-k_1}$

Now we achieve

$$Pr_1{}' = \Pr\left(f_{BA} > f_{th} | H_a > \frac{1+k_1}{1-k_1}H_b + \frac{k_2}{1-k_1}\right) \tag{20}$$

(b) If $H_a > H_b$, not overcome the influence of $p_{r1} > p_{r2}$, then $k > 1$,$f_{BA} > f_{AB}$

$$Pr_2{}'' = \Pr\left(f_{AB} > f_{th} | H_a > H_b > \frac{1-k_1}{1+k_1}H_a - \frac{k_2}{1+k_1}\right) \tag{21}$$

In conclusion, the outage probability is

$$Pr_1 = Pr_1{}' \tag{22}$$

$$Pr_2 = Pr_2{}' + Pr_2{}'' \tag{23}$$

$$\mathrm{Pr}_1{}' = \int_{f_{th}\left(5\sigma_E^2 + \frac{\mathrm{M}}{p_s} + \frac{1}{p_{r1}}\right)}^{\infty} \int_{\max\left\{\frac{p_s\sigma_E^2 h_b + \mathrm{M}\sigma_E^2 + 2p_s\sigma_E^4 + \frac{p_s h_b + \mathrm{M} + 2p_s\sigma_E^2}{p_{r1}}}{\frac{p_s h_b}{f_{th}} - 5p_s\sigma_E^2 - \mathrm{M} - \frac{p_s}{p_{r1}}}, \frac{(1+k_1)}{(1-k_1)}h_b + \frac{k_2}{(1-k_1)}\right\}}^{\infty} f_{H_a}\left(h_a\right)d\left(h_a\right)f_{H_b}\left(h_b\right)d\left(h_b\right) \tag{24}$$

p_{r1} is expressed as in Equation (20), where $f_{H_a}\left(h_a\right)$ and $f_{H_b}\left(h_b\right)$ are the probability density functions (PDF) of H_a and H_b, and $h_a, h_b \sim Exp\left(1/2\mu^2\right)$. E_M denotes the expectation operation. Considering the high SINR condition, the range of integration of h_a and h_b is in $(AH_{a/b} + B, \infty)$. Thus, we can rewrite the formula as Equation (25)

$$\mathrm{Pr}_1{}' \approx E_{\mathrm{M}}\left(\begin{array}{l}\left(\frac{1}{2} - \frac{1}{2}\frac{p_s\left(\frac{1}{p_{r2}} - \frac{1}{p_{r1}}\right)}{\mathrm{M}+4p_s\sigma_E^2}\right) * \exp\left(-\frac{1}{2\mu^2}\left(\frac{2p_s\sigma_E^2(f_{th}-1)\left(\frac{1}{p_{r2}} - \frac{1}{p_{r1}}\right) + \frac{p_s}{p_{r1}^2} + \frac{p_s}{p_{r2}}\left(\frac{1}{p_{r2}} - \frac{2}{p_{r1}}\right)}{\mathrm{M}+4p_s\sigma_E^2 - p_s\left(\frac{1}{p_{r2}} - \frac{1}{p_{r1}}\right)} + \frac{2f_{th}}{p_s}\mathrm{M}\right)\right) \\ * \exp\left(-\frac{1}{2\mu^2}\left(10f_{th}\sigma_E^2 + \frac{1}{p_{r2}} - \frac{1}{p_1} + \frac{2f_{th}}{p_{r2}}\right)\right)\end{array}\right) \tag{25}$$

Let $\mathrm{M} = \sum_{n=1}^{N} p_{I,n}\left|h_{I,n}\right|^2 = \sum_{n=1}^{N}\Omega_n$, where Ω_n exponential random variable and the parameter is $E\left[\Omega_n\right] = p_{I,n} = \nu_n$. We learn from reference [19] that the PDF of Ω_n is

$$f_M\left(m\right) = \sum_{i=1}^{\phi(\Omega)}\sum_{j=1}^{\varphi_i(\Omega)}\eta_{i,j}\left(\Omega\right)\frac{\left(\nu\left[i\right]\right)^{-j}}{\Gamma\left(j\right)}m^{j-1}e^{-\frac{m}{\nu[i]}} \tag{26}$$

where Ω represents the diagonal matrix with the elements v_n, $\phi(\Omega)$ is the number of different diagonal elements of matrix Ω. In addition, $\nu[i]$ denotes the ordered values of $\phi(\Omega)$ different elements which is $\nu[1] > \nu[2] > \cdots > \nu[\phi(\Omega)]$; $\phi_i(\Omega)$ is the number of replications of i_{th} element; $\eta_{i,j}(\Omega)$ is the character coefficient of matrix Ω. Then applied Equation (22) into Equation (21), get Equations (27) and (28).

$$\begin{aligned}\mathrm{Pr}_1 = F_M(m) \approx \sum_{i=1}^{\phi(\Omega)} \sum_{j=1}^{\varphi_i(\Omega)} \eta_{i,j}(\Omega) \frac{(\nu[i])^{-j}}{\Gamma(j)} * \exp\left(-\frac{1}{2\mu^2}\left(10 f_{th}\sigma_E^2 + \frac{1}{p_{r2}} - \frac{1}{p_{r1}} + \frac{2f_{th}}{p_{r2}}\right)\right) \\ * \int_0^\infty m^{j-1} e^{-\frac{m}{\nu[i]}} * \left(\frac{1}{2} - \frac{1}{2}\frac{p_s\left(\frac{1}{p_{r2}} - \frac{1}{p_{r1}}\right)}{m + 4p_s\sigma_E^2}\right) * \exp\left(-\frac{1}{2\mu^2}\left(\frac{2p_s\sigma_E^2(f_{th}-1)\left(\frac{1}{p_{r2}} - \frac{1}{p_{r1}}\right) + \frac{p_s}{p_{r1}^2} + \frac{p_s}{p_{r2}}\left(\frac{1}{p_{r2}} - \frac{2}{p_{r1}}\right)}{m + 4p_s\sigma_E^2 - p_s\left(\frac{1}{p_{r2}} - \frac{1}{p_{r1}}\right)} + \frac{2f_{th}}{p_s}m\right)\right) dm\end{aligned} \tag{27}$$

$$\begin{aligned}\mathrm{Pr}_2 = F_M(m) \approx \sum_{i=1}^{\phi(\Omega)} \sum_{j=1}^{\varphi_i(\Omega)} \eta_{i,j}(\Omega) \frac{(\nu[i])^{-j}}{\Gamma(j)} * \exp\left(-\frac{1}{2\mu^2}\left(10 f_{th}\sigma_E^2 + \frac{1}{p_{r1}} - \frac{1}{p_{r2}} + \frac{2f_{th}}{p_{r1}}\right)\right) \\ * \int_0^\infty m^{j-1} e^{-\frac{m}{\nu[i]}} * \left(\frac{1}{2} + \frac{1}{2}\frac{p_s\left(\frac{1}{p_{r2}} - \frac{1}{p_{r1}}\right)}{m + 4p_s\sigma_E^2}\right) * \exp\left(-\frac{1}{2\mu^2}\left(\frac{2p_s\sigma_E^2(1-f_{th})\left(\frac{1}{p_{r2}} - \frac{1}{p_{r1}}\right) + \frac{p_s}{p_{r2}^2} + \frac{p_s}{p_{r1}}\left(\frac{1}{p_{r1}} - \frac{2}{p_{r2}}\right)}{m + 4p_s\sigma_E^2 + p_s\left(\frac{1}{p_{r2}} - \frac{1}{p_{r1}}\right)} + \frac{2f_{th}}{p_s}m\right)\right) dm\end{aligned} \tag{28}$$

Above all, outage probability of the network can be expressed in Equation (29):

$$P_{out} = 1 - Pr_1 - Pr_2 \tag{29}$$

$$\mathrm{Pr}_1 = \mathrm{Pr}_2 = \frac{1}{2}\exp\left(-\frac{1}{\mu^2}\left(5 f_{th}\sigma_E^2 + \frac{f_{th}}{p_r}\right)\right) * \sum_{i=1}^{\phi(\Omega)} \sum_{j=1}^{\varphi_i(\Omega)} \eta_{i,j}(\Omega) * \left(1 + \frac{f_{th} * \nu[i]}{\mu^2 p_s}\right)$$

First, it should be noted that if $p_{r1} = p_{r2} = p_r$, Equations (27) and (28) can be simplified as equal to the consequence of reference [13] (Equation (18)). Second, note that p_{r1} and p_{r2} are very similar in most cases, but not equal. They are all affected by target rate f_{th} and the difference of the reciprocals of two relay emission powers. When the signal power p_s is strong enough, the difference of the reciprocals of two relay emission powers will not be the main influence factor.

4. Theoretical Calculation and Simulation Analysis

In Section 4, we verify above theoretical analysis by data simulation. The simulation diagram and parameters are shown in Figure 4 and Table 1. The hierarchical heterogeneous network model is shown in Figure 5, where the green squares represent macro cells, the red squares represent randomly distributed micro cells, and the blue squares represent users. The network also provides two user connection modes: (a) Both users access a random macro cell; (b) Both users access a random micro cell. It is possible to simulate the access mode of two users and perform system performance studies in the selected mode.

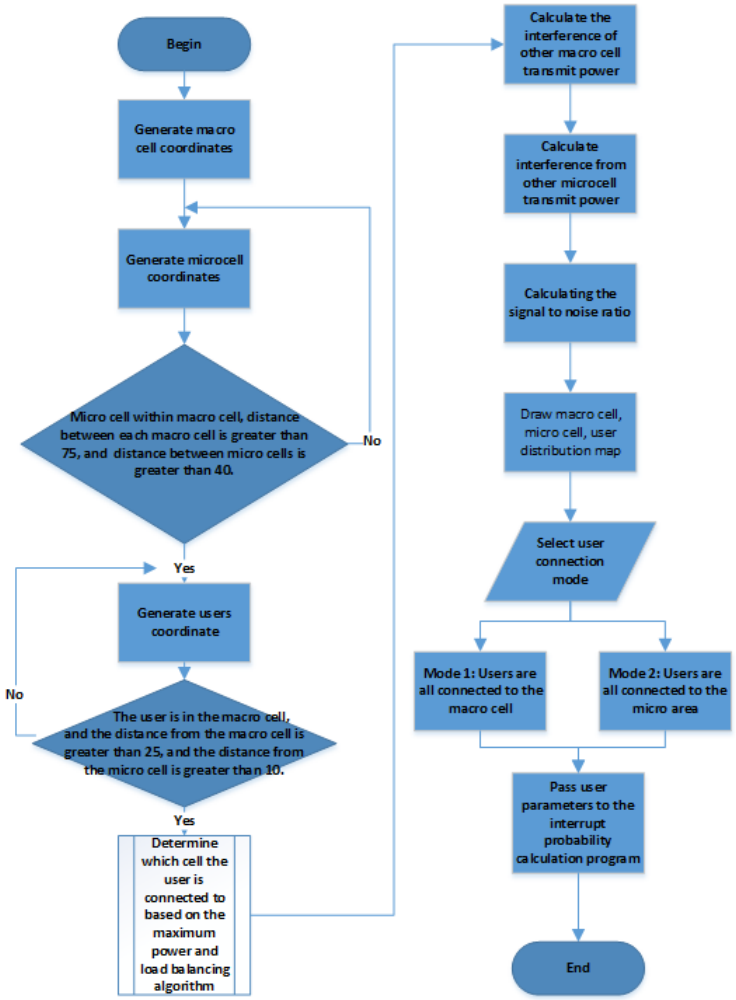

Figure 4. System simulation diagram.

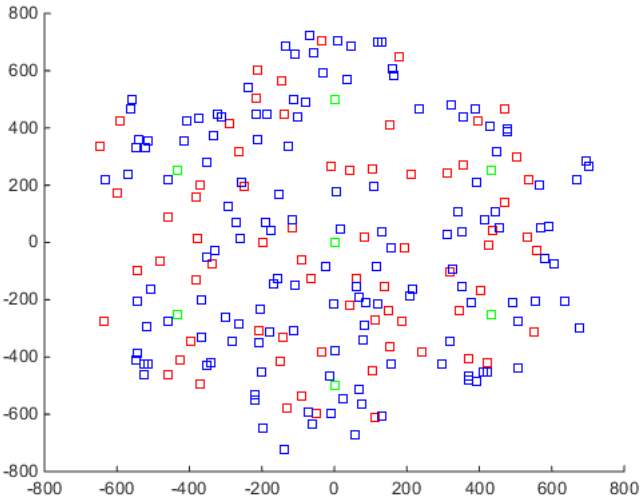

Figure 5. Hierarchical heterogeneous network model (7 macro cells, 70 micro cells, 140 users).

Table 1. Simulation parameters.

Environmental Deployment	10 Micro Cells Randomly Distributed Around Macro Cell
Cell Connection Plan	RSRP and CL
Bandwidth	10 MHz
Carrier Frequency	2 GHz
Path Loss Model	3 GPP TR 36.814 Model 1
Distance between Macro cells	250 m
Maximum Macro Cell Transmit Power	46 dBm
Maximum Micro Cell Transmit Power	30 dBm
Noise Figure	9 dB
Macro cell eNodeB Antenna Model	3D Antenna Model
Micro Cell eNodeB Antenna Model	Omnidirectional Antenna, 2D Antenna Model
Macro Cell Antenna Gain	14 dBi
Micro Cell Antenna Gain	5 dBi
Antenna Configuration	2 Cross-polarized Transmit Antennas for eNodeBs
Receiver Type	Minimum Mean Square Error Receiver
Minimum Distance Between Micro cell and Macro cell	75 m
Minimum Distance Between Micro Cells	40 m
Minimum Distance Between Macro cell and user	25 m
Minimum Distance Between Micro cell and user	10 m

In Figure 6, with the variance of channel estimation errors, we set up the number of interferers $N = 4$ and the powers of N interferers $u_1 = 2.1$, $u_2 = 0.5$, $u_3 = 6$, $u_4 = 1.4$, respectively. The target threshold f_{th} is 5 dB. Consequently, the comparison of the outage probability results of the analytical Equation (19) in [13], the aforementioned Equation (29), and the data simulation are illuminated in Figure 4. It is obvious to see that the theoretical results of Equations (19) and (29) are very approximate at low relay power, and as the relay power increases, their performance shows some difference; even though the simulation results have similar trends to theoretical analysis, there is a gap in comparison with theoretical values.

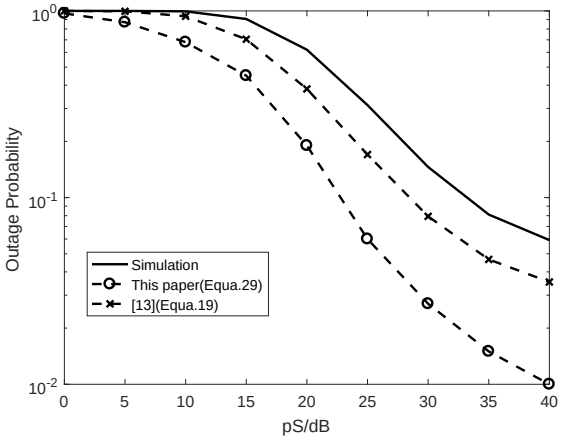

Figure 6. Outage probability of HHWN with MMR of different emission powers.

Figure 7 displays the system outage probability results with different power ratios, i.e., the p_{r2} equals to 9/10, 1/2, 1/3, 1/4, 1/5 times p_{r1}, respectively. As we see in results, there is little difference between the analytical results of different emission power p_{r2} size. Then with the increase of p_s, there are differences between them, but they all show some differences gradually, which means that

the multiplicative between two emission powers (p_{r1} and p_{r2}) will not have significant influence on the outage probability.

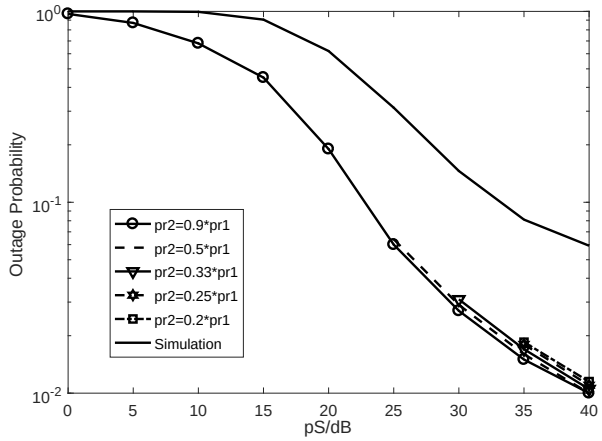

Figure 7. Outage probability of HHWN with MMR as different relay power p_{r2} equals 9/10,1/2,1/3,1/4,1/5 times p_{r1}.

Figure 8 depicts the system spectral efficiency (SE) with different power ratios. The solid, dashed, triangle, rhombus, square, and star lines indicate SE of $p_{r2} = \lambda * p_{r1}, \lambda = 1, 9/10, 1/2, 1/3, 1/4, 1/5$, respectively. As shown in the figure, the base line is $p_{r2} = p_{r1}$ and the other SEs of HHWN system decreases when the power gap grows. When SE is more than 4 bits/s/Hz, the gap between $p_{r2} = p_{r1}$ and $p_{r2} = 0.25 * p_{r1}$ reaches 3 dB. Consequently, to avoid 3 dB loss of SE, the power ratio should be higher than 0.25.

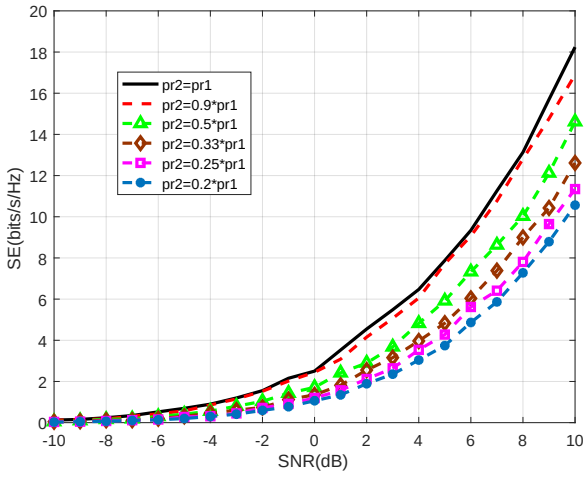

Figure 8. Spectral efficiency of HHWN with MMR as different relay power p_{r2} equals 9/10,1/2,1/3,1/4,1/5 times p_{r1}.

Figure 9 displays the performance of system outage probability, which is plotted by using Equation (29) in the circumstance with different noise power: $p_n = \sigma_E^2 = 10^{-2}, 10^{-3}, 10^{-4}, 10^{-5}, 10^{-6}$, respectively. We can observe that the power level of noise significantly affects the system performance. Notice that when $p_n = 10^{-2}$, the simulation results are approximate with the theoretical value before p_s reaches 28 dB. One interesting point is that with the increase of p_s, the system performance grows better than the theoretical analysis to a certain extent.

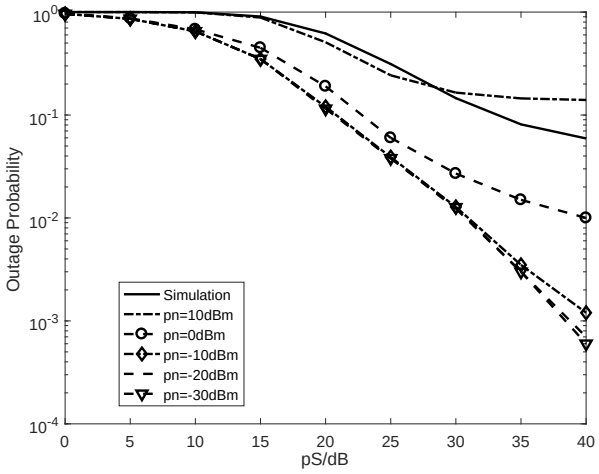

Figure 9. Outage probability of HHWN with MMR as different noise power $p_n = \sigma_E^2 =$ 10 dBm, 0 dBm, −10 dBm, −20 dBm, −30 dBm.

5. Conclusions

In this paper, we applied the multi-mode relay (MMR) model based on two-way relay technology to heterogeneous hierarchical wireless networks (HHWN), and set up a system model of HHWN. Then, we considered the system with unequal relay emission powers situation, by defining the two-way SINR ratio factor, deriving the mathematical formulas of outage error probability with channel estimation errors. Theoretical results and data simulation demonstrate the qualitative influence on the system with different levels of relay emission power from MMR to different UEs nodes and noises. Several comparison works are implemented for different schemes.

Author Contributions: Conceptualization, W.B. and Y.X.; Methodology, W.B.; Software, Y.X.; Formal analysis, W.B. and Y.X.; Writing—original draft preparation, Y.X.; Writing—review and editing, W.B.; Funding acquisition, D.H., Y.Z.

Funding: This research was funded by the National Natural Science Foundation of China (No. 61371143), Beijing Natural Science Foundation—Haidian Original Innovation Joint Fund Project Task Book (No. L182039), Industrial-university Cooperation and Collaborative Education Project for Higher Education Department of the Ministry of Education (No. 201801121002), Project of 2019 for Association of Computing Education in Chinese Universities (No. CERACU2019R05).

Conflicts of Interest: The authors declare no conflict of interest.

References

1. Molisch, A.F.; Ratnam, V.V.; Han, S.; Li, Z.; Nguyen, S.L.H.; Li, L.; Haneda, K. Hybrid beamforming for massive MIMO: A survey. *IEEE Commun. Mag.* **2017**, *55*, 134–141. [CrossRef]
2. Ahmed, I.; Khammari, H.; Shahid, A.; Musa, A.; Kim, K.S.; De Poorter, E.; Moerman, I. A survey on hybrid beamforming techniques in 5G: Architecture and system model perspectives. *IEEE Commun. Surv. Tutor.* **2018**, *20*, 3060–3097. [CrossRef]
3. Xiao, Y.; Wang, Y.; Xiang, W. Dimension-Deficient Channel Estimation of Hybrid Beamforming Based on Compressive Sensing. *IEEE Access* **2019**, *7*, 13791–13798. [CrossRef]
4. Ghosh, A.; Andrews, J. Heterogeneous Cellular Networks: From Theory to Practice. *IEEE Commun. Mag.* **2012**, *50*, 54–64. [CrossRef]
5. Hasnat, M.A.; Rumee, S.T.A.; Razzaque, M.A.; Mamun-Or-Rashid, M. Security Study of 5G Heterogeneous Network: Current Solutions, Limitations & Future Direction. In Proceedings of the 2019 International Conference on Electrical, Computer and Communication Engineering (ECCE), Cox'sBazar, Bangladesh, 7–9 February 2019; pp. 1–4.

6. Zhang, J.; Bai, W.; Wang, Y. Non-interactive ID-based Proxy Re-signature Scheme for IoT Based on Mobile Edge Computing. *IEEE Access* **2019**, *7*, 37865–37875. [CrossRef]
7. Shen, Y.; Pei, Q. HGRP: Hybrid Grid Routing Protocol for Heterogeneous Hierarchical Wireless Networks. In Proceedings of the Third International Conference on Intelligent Networking and Collaborative Systems, Fukuoka, Japan, 30 November–2 December 2011.
8. Zhang, H.; Jiang, C.; Cheng, J. Cooperative interference mitigation and handover management for heterogeneous cloud small cell networks. *IEEE Wirel. Commun.* **2015**, *22*, 92–99. [CrossRef]
9. Mamun, M.; Yuji, K. HEHC: Heterogeneous-Aware Enhanced Hierarchical Clustered Scheme for Wireless Sensor Networks. In Proceedings of the SICE Annual Conference, Tokyo, Japan, 13–18 September 2011.
10. Zhang, H.; Jiang, C.; Beaulieu, N.; Chu, X.; Wen, X.; Tao, M. Resource Allocation in Spectrum-Sharing OFDMA Femtocells With Heterogeneous Services. *IEEE Trans. Commun.* **2014**, *62*, 2366–2377. [CrossRef]
11. Zhang, H.; Chu, X.; Guo, W.; Wang, S. Coexistence of Wi-Fi and heterogeneous small cell networks sharing unlicensed spectrum. *IEEE Commun. Mag.* **2015**, *53*, 158–164. [CrossRef]
12. Li, B.; Shi, W. A Hierarchical Semi-Centralized Architecture for Load Balancing of Heterogeneous Wireless Networks. In Proceedings of the 2010 Second International Conference on Networks Security, Wireless Communications and Trusted Computing, Wuhan, China, 24–25 April 2010.
13. Yang, L.; Qaraqe, K. Performance Analysis of Amplify-and-Forward Two-Way Relaying with Co-Channel Interference and Channel Estimation Error. *IEEE Trans. Commun.* **2013**, *61*, 2221–2231. [CrossRef]
14. Zhang, H.; Xing, H.; Cheng, J.; Nallanathan, A.; Leung, V. Secure Resource Allocation for OFDMA Two-Way Relay Wireless Sensor Networks Without and With Cooperative Jamming. *IEEE Trans. Ind. Inform.* **2016**, *12*, 1714–1725. [CrossRef]
15. Peng, M.; Liu, Y.; Wei, D.; Wang, W. Hierarchical Cooperative Relay Based Heterogeneous Networks. *IEEE Wirel. Commun.* **2011**, *18*, 48–56. [CrossRef]
16. Dhillon, H.; Andrews, J. Modeling and Analysis of K-Tier Downlink Heterogeneous Cellular Networks. *IEEE J. Sel. Areas Commun.* **2012**, *30*, 550–560. [CrossRef]
17. Ikki, S.S.; Aissa, S. Performance analysis of two-way amplifyand-forward relaying in the presence of co-channel interference. *IEEE Trans. Commun.* **2012**, *60*, 933–939. [CrossRef]
18. Da Costa, D.B.; Ding, H.; Yacoub, M.D.; Ge, J. Outage Analysis of Two-way relaying in interference-limited AF cooperative networks over Nakagami-m fading. *IEEE Trans. Veh. Technol.* **2012**, *61*, 3766–3771. [CrossRef]
19. Zhong, C.; Jin, S.; Wong, K.-K. Dual-hop systems with noisy relay and interference-limited destination. *IEEE Trans. Commun.* **2010**, *58*, 764–768. [CrossRef]